Molecular Therapy
Nucleic Acids
Original Article

Secondary follicles enable efficient germline mtDNA base editing at hard-to-edit site

Qin Xie,[1,4] Haibo Wu,[1,4] Hui Long,[1,4] Caiwen Xiao,[2,3,4] Jiaxin Qiu,[1,4] Weina Yu,[1,4] Xueyi Jiang,[1] Junbo Liu,[1] Shuo Zhang,[1] Qifeng Lyu,[1] Lun Suo,[1] and Yanping Kuang[1]

[1]Department of Assisted Reproduction, Shanghai Ninth People's Hospital, Shanghai Jiao Tong University School of Medicine, Shanghai 200011, China; [2]Department of Ophthalmology, Ninth People's Hospital, Shanghai Jiao Tong University School of Medicine, Shanghai 200011, China; [3]Shanghai Key Laboratory of Orbital Diseases and Ocular Oncology, Shanghai 200011, China

Efficient germline mtDNA editing is required to construct disease-related animal models and future gene therapy. Recently, the DddA-derived cytosine base editors (DdCBEs) have made mitochondrial genome (mtDNA) precise editing possible. However, there still exist challenges for editing some mtDNA sites in germline via zygote injection, probably due to the suspended mtDNA replication during preimplantation development. Here, we introduce a germline mtDNA base editing strategy: injecting DdCBEs into oocytes of secondary follicles, at which stage mtDNA replicates actively. With this method, we successfully observed efficient G-to-A conversion at a hard-to-edit site and also obtained live animal models. In addition, for those editable sites, this strategy can greatly improve the base editing efficiency up to 3-fold, which is more than that in zygotes. More important, editing in secondary follicles did not increase more the risk of off-target effects than that in zygotes. This strategy provides an option to efficiently manipulate mtDNA sites in germline, especially for hard-to-edit sites.

INTRODUCTION

The mitochondria are important organelles, serving as the power plants of the cell and playing important roles in cellular metabolism.[1,2] Within the mitochondrial genome (mtDNA), a total of 37 genes encode essential proteins and RNAs for the oxidative respiratory chain.[3] Mutations in crucial regions of mtDNA can result in mitochondrial dysfunction and serious diseases.[4,5] Recently, hundreds of pathogenic sites in human mtDNA have been clinically confirmed (www.mitomap.org). Unfortunately, appropriate disease models are lacking, and therapeutic methods for these diseases are extremely rare.[3]

For heritable nuclear genetic disease, the germline DNA editing technique of injecting editors into zygotes is a common method for constructing disease-relevant animal models.[6] This technique plays a critical role in clarifying the relationship between inherited mutations and disease phenotypes. Furthermore, germline gene editing-mediated correction of disease-causing mutations could act as a promising option for preventing transmission of these diseases between generations.[3,7] However, unlike the nuclear genome, mtDNA editing is difficult using the classic CRISPR-Cas9 method due to challenges in delivering single-guide RNAs into the mitochondrial matrix and repairing double-strand breaks in mtDNA.[8–10] Recently, two single-strand-independent and CRISPR-free base editing tools, called DddA-derived cytosine base editors (DdCBEs) and transcription activator-like effector (TALE)-linked deaminases, have been developed.[11,12]

Among them, DdCBEs use each TALE monomer to target a specific sequence in the mtDNA and use split DddA halves to efficiently catalyze C·G to T·A conversion. It has been successfully used to modify mtDNA in cultured mammalian cells[11] and embryos of commonly used model animals, including zebrafish,[13] rat,[14,15] and mice,[16,17] as well as human embryos.[18,19] However, the editing efficiency in germ cells was found to be much lower than in somatic cells,[13,14,17,19] and some mtDNA sites that were easily edited in somatic cells could not be edited in germ cells through zygote injection.[14,19]

Here, we propose a germline mtDNA base editing strategy that injects DdCBEs into oocytes of secondary follicles. This strategy could not only overcome the challenges of editing hard-to-edit sites in germline but also greatly enhance the editing efficacy for those editable sites.

Received 3 March 2023; accepted 8 March 2024;
https://doi.org/10.1016/j.omtn.2024.102170.

[4]These authors contributed equally

Correspondence: Qifeng Lyu, Department of Assisted Reproduction, Shanghai Ninth People's Hospital, Shanghai Jiao Tong University School of Medicine, Shanghai 200011, China.
E-mail: lvqf3327@sh9hospital.org.cn
Correspondence: Lun Suo, Department of Assisted Reproduction, Shanghai Ninth People's Hospital, Shanghai Jiao Tong University School of Medicine, Shanghai 200011, China.
E-mail: 314005@sh9hospital.org.cn
Correspondence: Yanping Kuang, Department of Assisted Reproduction, Shanghai Ninth People's Hospital, Shanghai Jiao Tong University School of Medicine, Shanghai 200011, China.
E-mail: kuangyp1506@sh9hospital.org.cn

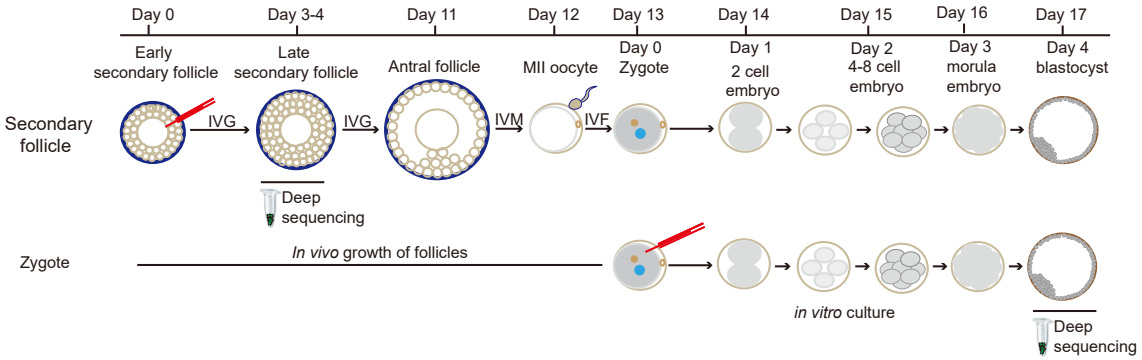

Figure 1. Flowchart of DdCBE injection in zygotes and secondary follicles

RESULTS

Secondary follicles enable efficient germline mtDNA base editing

We first set up an *in vitro* follicle culture system based on a previously reported method.[20] In brief, secondary follicles were isolated from 12- to 14-day-old mice and injected with DdCBEs. The follicles were then cultured for 11 days for oocyte growth. When the cumulus-oocyte complexes (COCs) are differentiated, the COCs are collected and subjected to *in vitro* maturation followed by *in vitro* fertilization. The procedure for injection is shown in Video S1. In parallel, zygotes obtained from 6- to 8-week-old mice were also subjected to DdCBE injection. These manipulated zygotes were then subjected to a 4-day culture for blastocyst formation (Figure 1).

DdCBEs mediated mtDNA base editing depends on mtDNA replication.[11] To initiate base editing, DdCBEs first convert cytosine to uracil within double-stranded DNA, and the uracil will be substituted with thymine through the mtDNA replication process.[11] Therefore, we quantified the mtDNA copy number of germ cells at different developmental stages. The results indicated that either the mtDNA copy number or the copy number shift remained stable or even slightly decreased during preimplantation embryonic development (Figures 2A and 2B), whereas the copy number of mtDNA increased by about 40% during the early-secondary follicle development from days 1 to 3 cultured *in vitro* (Figures 2C and 2D), which exhibited a huge potential of secondary follicle for improving the efficiency of mtDNA base editing.

To test the feasibility of this hypothesis, one mtDNA site, mt-Nd1 m.G3177 in mice, corresponding to human MT-ND1 m.G3733-confirmed mutation site for Leber hereditary optic neuropathy (LHON; m.3733 G>A), was used as a candidate site (Table S1). Then, four kinds of TALE nuclease (TALEN)-based DddAtox pairs (L1333N-R1333C, L1333C-R1333N, L1397N-R1397C, and L1397C-R1397N) were designed, constructed, and transfected into Neuro-2A cells to test their base editing efficiency. Six days posttransfection, two G1397 pairs showed adequate editing efficiency as high as ~30% (Figures 3A and 3B), and the editing efficiency of different sites within the spacer region for each pair is shown in Figure S1A. However, when mt-Nd1-DdCBE mRNAs from the optimal pair (L1397C-R1397N) were injected into zygotes, no detectable mutation was identified by the Sanger sequence at first (Figure 3C). To figure out whether a rare mutant occurred in zygotes, we used digital PCR to detect the rare mutation copies and the results indicated that the average mutant rate is only 0.04% (from 0 to 0.17%) in zygotes (Figure 3D). Remarkably, when we injected mt-Nd1-DdCBE mRNA into expanded germinal vesicle (GV) oocytes (fully grown oocytes) and oocytes of secondary follicles (growing oocytes) (Figures S2A and S2B), the ratio of mutant variants increased obviously, especially in oocytes of the secondary follicles with a C·G to T·A conversion rate as high as 28.78% (from 5.70 to 28.78%, average rate 15.92%) (Figures 3C, 3D, and S2C). More important, increased on-target editing efficiency did not induce an unexpected conversion of nontarget cytosine within the spacer region in secondary follicles (Figure S1B). To further validate the reliability of this method, another pair of DddAtox (L1397N-R1397C) was also injected into zygotes or oocytes of the secondary follicles. The digital PCR results showed similar results that the secondary follicles also obtained the optimal editing efficiency, whereas the mtDNA of zygotes was still hardly edited (Figure S3). These results indicated that germline mtDNA editing performed at secondary follicles could serve as a potential choice for the conventionally hard-to-edit site.

Besides the above hard-to-edit site, we tested the efficacy of this method for those editable sites with a recently reported site mt-Nd5 m.G12918 (Table S1). The optimal DddAtox pair (L1397N-R1397C) was selected from the four kinds of TALEN-based pairs (Figures 3E, 3F, and S1C). Similarly, we found that secondary follicles induced higher editing efficiency (4.47%–44.73%, average: 31.85%) at the m.G12918 site, which was over 3-fold higher than the zygotes (1.90%–19.90%, average: 9.52%) (Figures 3G and 3H). Furthermore, editing at secondary follicles did not induce nontargets within the spacer region (Figure S1D). These results showed that secondary follicles not only enabled efficient base editing for the hard-to-edit site but also greatly improved base editing efficiency for the conventionally editable site.

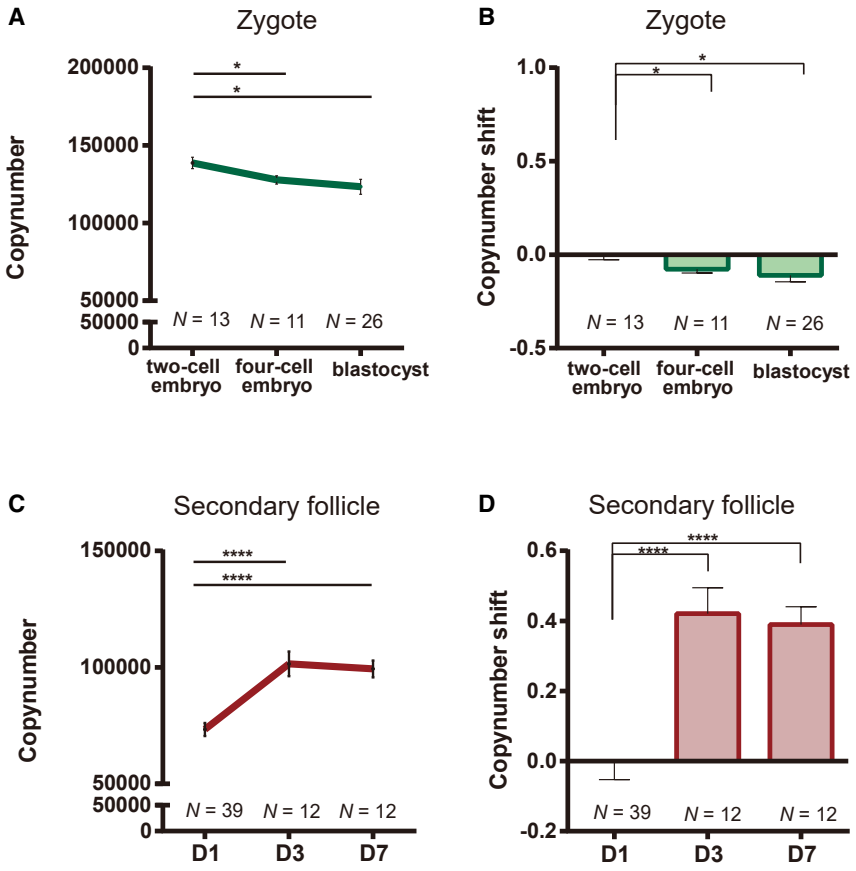

Figure 2. Dynamics of mtDNA copy number during preimplantation embryo and *in vitro* cultured secondary follicles development

(A and C) The copy number of mtDNA during *in vitro* cultured preimplantation embryo development (A) and *in vitro* cultured follicles (C). (B and D) The copy number shift of mtDNA during *in vitro* cultured preimplantation embryos (B) and *in vitro* cultured follicles (D). Significance was calculated with unpaired two-tailed Student's t test or Mann-Whitney *U* test as appropriate (*p < 0.05; ****p < 0.0001). The error bars represent the standard error of the mean.

Whole mitochondrial genome-wide off-targets post DdCBE-mediated mtDNA editing in secondary follicles

Other than the editing efficiency, minimizing off-targeting is another key factor affecting the applications of gene editing techniques.[21] To investigate the number of off-targets, whole mtDNA genome sequencing was performed. For both mt-Nd1- and mt-Nd5-DdCBE, the average C·G to T·A conversion of mitochondrial genome-wide off-targets was comparable between secondary follicles and zygotes, which indicated that editing performed at secondary follicles did not increase the risks of off-targets in the mitochondrial genome (Figures 4A and 4B). In particular, an unexpected off-target site with a 3.43%–5.17% mutation rate has been shown in 2/3 zygotes injected with mt-Nd1-DdCBE even when the on-target efficiency is below the sensitivity of the NGS technical limitation. Meanwhile, no obvious off-target site has been shown in secondary follicles injected with mt-Nd1-DdCBE, whereas the editing efficiency of the on-target site was as high as 14.44%–27.12% (Figures 4C, 4D, and S4). For mt-Nd5-DdCBE, zygotes showed no obvious off-targets and 2/3 secondary follicles showed only 1 off-target with a 5.27%–9.38% mutation rate (Figures 4C, 4E, and S5). All of the results above suggested that high editing efficiency and no obvious off-target made secondary follicle a potential and promising stage for germline mtDNA editing.

Developmental potential of the oocytes derived from the edited secondary follicles

For assessing the developmental potential of the oocytes derived from the edited secondary follicles, secondary follicles were cultured *in vitro* for 11 days, and the expanded COCs were fertilized. A total of 14 blastocysts were obtained from 50 untreated secondary follicles cultured *in vitro* (28.0%), and 6 blastocysts were obtained from 60 mt-Nd1-DdCBE edited secondary follicles (10.0%) (Table 1). We speculated that mtDNA carrying disease-related mutation may impair the developmental potential of edited oocytes. When 82 two-cell stage embryos derived from injected follicles were transferred into the oviducts of pseudopregnant females, two live pups were obtained with the efficiency of G-to-A conversion up to 14.57% (3.4%–25.70%). Meanwhile, the mean editing efficiency of the five live pups derived from zygotes is only 0.24% (ranging from 0.06% to 0.41%). Moreover, when the mutation frequency was tested in various tissues from this adult F0 mouse at 5 months postbirth, the result indicated that mtDNA heteroplasmy among different tissues is equivalent and without the mosaicism (Figure 5).

Evaluation of visual evoked potential (VEP) in wild-type (WT) and m.3177 G>A models

Despite showing no outward LHON symptoms such as blindness, we investigated potential optic nerve effects of the m.3177 G>A mutation in these mice. VEP examinations, sensitive to optic nerve function, revealed significantly lower amplitudes in LHON mice compared to their (WT) counterparts (Figure 6). This finding, consistent with typical LHON presentations in which compromised optic nerve axons lead to reduced VEP amplitude, suggests potential visual processing impairment likely due to factors such as reduced retinal ganglion cell activity and impaired synaptic transmission.

DISCUSSION

Unlike the nuclear genome with only two copies in one cell, the mitochondria genome (mtDNA) contains thousands of mtDNA copies in one somatic cell or even hundreds of thousands of copies

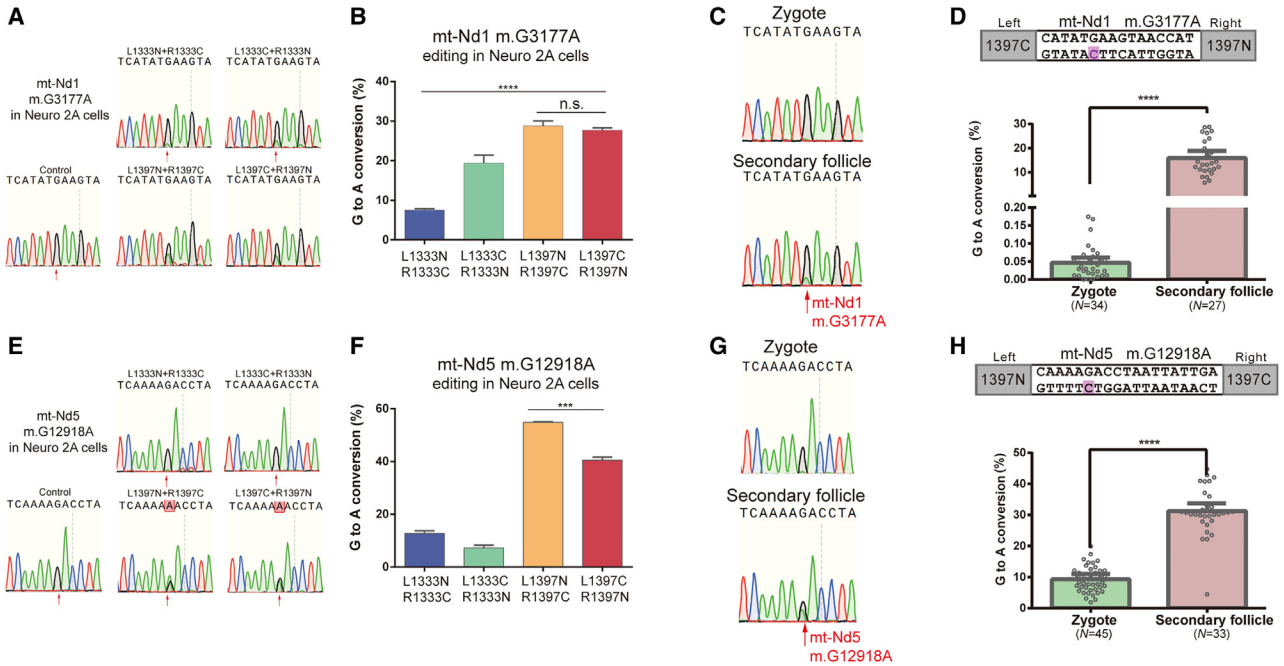

Figure 3. DdCBE-mediated mtDNA base editing in Neuro-2A cells, zygotes and secondary follicles

(A) Confirmation of mt-Nd1-DdCBE mediated mtDNA editing by Sanger sequence in Neuro-2A cells with 4 kinds of DddAtox pairs. The target site is indicated by the red arrow. (B) Comparison of the editing efficiency of mt-Nd1-DdCBE mediated mtDNA editing in Neuro-2A cells with 4 kinds of DddAtox pairs by NGS. (C) Sanger sequence results of zygotes and secondary follicles 4 days after injection of mt-Nd1-DdCBE mRNAs. The target site is indicated by the red arrow. (D) Comparison of the mtDNA base editing efficiency of zygotes and secondary follicles 4 days after injection of mt-Nd1-DdCBE mRNAs. (E) Confirmation of mt-Nd5-DdCBE mediated mtDNA editing by Sanger sequence in Neuro-2A cells with 4 kinds of DddAtox pairs. The target site is indicated by the red arrow. (F) Comparison of the editing efficiency of and mt-Nd5-DdCBE mediated mtDNA editing in Neuro-2A cells with 4 kinds of DddAtox pairs by NGS. (G) Sanger sequence results of zygotes and secondary follicles 4 days after injection of mt-Nd5-DdCBE mRNAs. The target site is indicated by the red arrow. (H) Comparison of the mtDNA base editing efficiency of zygotes and secondary follicles 4 days after injection of mt-Nd5-DdCBE mRNAs. Significance was calculated with unpaired two-tailed Student's t test or Mann-Whitney *U* test as appropriate (ns, not significant; ***$p < 0.001$; ****$p < 0.0001$). The error bars represent the standard error of the mean.

in a single oocyte. Mitochondrial diseases occur only when the mutation load exceeds a certain threshold level. Therefore, the efficiency of mtDNA base editing should be high enough to reach the onset threshold for building a disease model or to relieve symptoms in gene therapy. Unfortunately, the current strategy that performs germline mtDNA editing at the zygote stage may not meet this demand. Furthermore, some mtDNA sites are still hard to edit in germline.[14,19]

The editing process starts from DddA-induced deamination, which catalyzes the conversion of cytosine to uracil and subsequently substitutes uracil with thymine. Importantly, this process relies on mtDNA replication.[11] However, previous studies have pointed out that during the early stage of embryo development, both in humans[22] and model animals,[23,24] mtDNA replication remains suspended. To address the challenge of improving editing efficiency in germline, we made a thorough investigation into the entire germline development process. A primordial germ cell undergoes a series of stages, including primary follicle, secondary follicle, antral follicle, zygote, early embryo, and fetus. During these stages, the mtDNA replication occurs before the antral follicle and after the morula embryo stage.[24] Accordingly, previous studies tried to delay the "editing window" until mtDNA started replication; a transposon was used in rat embryos[14] and DdCBEs were injected at the 8-cell stage in human embryos.[19] However, the transposon could increase the potential risk of mosaicism (the heteroplasmy of different tissues varied from ~5% to 15%),[14] and the 8-cell injection requires superior skills.[19] To minimize the risk of mosaicism, it may be a better choice to complete the editing process in a single cell with active mtDNA replication. We speculated that secondary follicles or GV oocytes (from antral follicles) could be a feasible option for efficient germline mtDNA editing.

Based on the above hypothesis, we injected DdCBEs into zygotes, GV oocytes, and oocytes of secondary follicles. We observed a correlation between editing efficiency and mtDNA replication. Specifically, secondary follicles with the most mtDNA replication exhibited the highest editing efficiency, GV oocytes with slight mtDNA replication exhibited moderate editing efficiency, and embryos with hard mtDNA replication exhibited the lowest editing efficiency.

Although secondary follicle editing did not raise the overall off-target risk, a single off-target from mt-Nd5-DdCBE highlights the potential

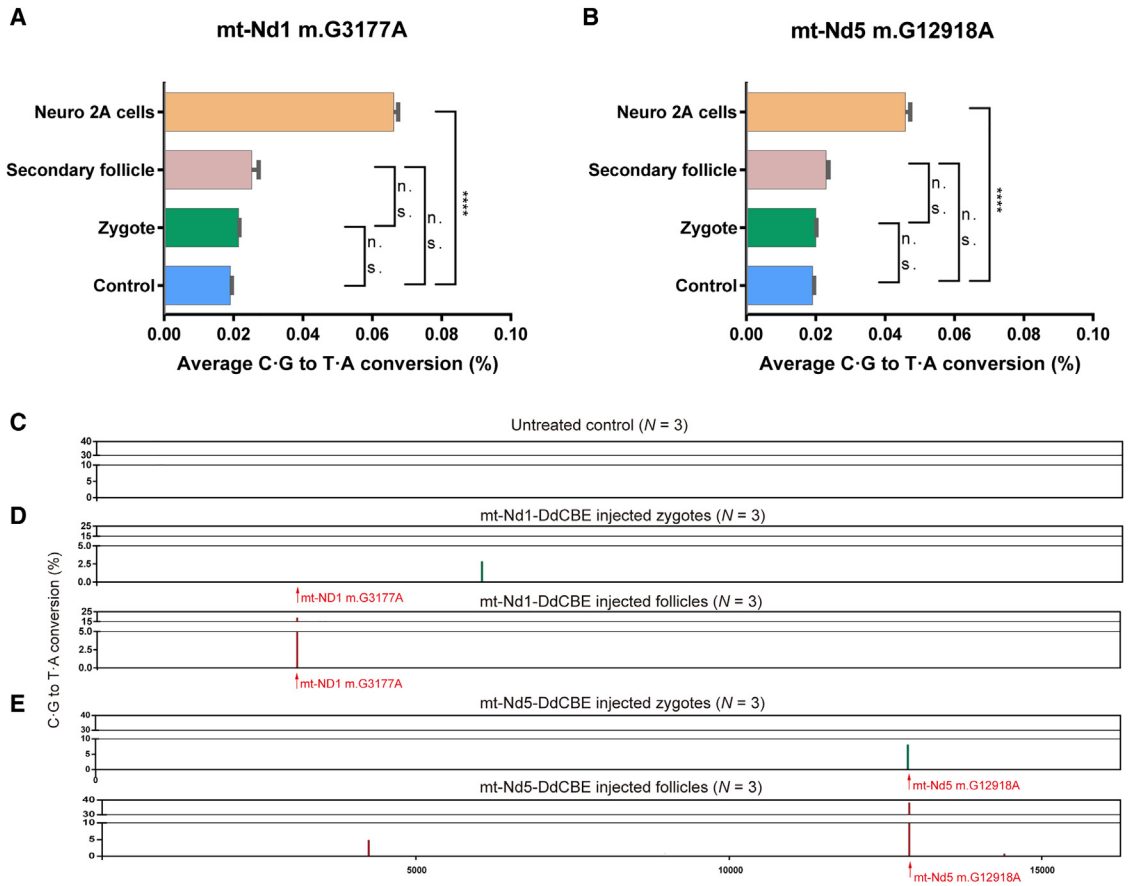

Figure 4. Off-target analysis of whole mtDNA genome post-mtDNA editing

(A) Average frequency of mtDNA-wide off-target C·G to T·A conversions for control, Neuro-2A cells, zygotes and secondary follicles post mt-Nd1-DdCBE mediated mtDNA editing. (B) Average frequency of mtDNA-wide off-target C·G to T·A conversions for control, Neuro-2A cells, zygotes and secondary follicles post mt-Nd5-DdCBE mediated mtDNA editing. (C–E) Frequencies of on- and off-target C·G to T·A conversion along the whole-mtDNA genome of embryos and oocytes derived from untreated control (C), mt-Nd1-DdCBE (D), and mt-Nd5-DdCBE (E) injected zygotes and secondary follicles, respectively. Significance was calculated with unpaired two-tailed Student's t test (****$p < 0.0001$). The error bars represent the standard error of the mean.

for possible effects. However, successful on-target editing without off-targets was also observed (Figure S5D), suggesting the possibility of selective breeding for cleaner models. Moreover, ongoing efforts such as optimized TALEN structures aiming to minimize off-target effects could also unlock the efficient mtDNA editing.

It should be noted, however, that the efficiency of obtaining live births from follicles cultured *in vitro* is not yet comparable to that from zygotes. Fortunately, as we know, *in vitro* oocyte development and maturation are key areas of future research in the field of reproduction due to their huge potential for applications.[25,26] A recent study in Japan has shown that *in vitro* cultured follicles can achieve blastocyst formation rates as high as 84.1% in model animals,[20] indicating that the limitation will be overcome in the near future. Besides its potential application in disease-related model construction and future gene therapy, this strategy provides a powerful research platform for studying the influence of mitochondria on follicle development. Mitochondria play an important role in oogenesis, and mutations in mtDNA can impair oogenesis and reproductive outcomes.[27,28] In line with these studies, our results suggest that oocytes with mutant mtDNA have lower developmental potential in oogenesis but potential in early embryo development comparable to that of oocytes without mtDNA mutation. Nonetheless, the underlying mechanisms are still unclear and worth further investigation.

Taken together, our germline mtDNA base editing strategy—injecting DdCBEs into oocytes of secondary follicles—highly improved the mtDNA editing efficiency in germline, especially for the hard-to-edit site. Together with assisted reproduction technologies, such as follicle *in vitro* culture followed by *in vitro* fertilization, it could serve as a potential medical option for correcting disease-causing mtDNA mutations in germline, thereby preventing the transmission of mitochondrial diseases between generations.

Table 1. Summary of the development potential of oocytes derived from secondary follicles with or without mt-Nd1-DdCBE injection

	No. of cultured follicles	No. of collected COCs	No. of oocytes matured into MII	No. of normally fertilized oocytes	No. of two-cell embryos	No. of blastocysts
Control follicles	50	46 (92.0% per follicles)	40 (80.0% per follicles; 87.0% per COCs)	31 (62.0% per follicles; 77.5% per MII oocytes)	31 (62.6% per follicles; 100% per fertilized oocytes)	14 (28.0% per follicles; 45.2% per 2-cell embryos)
mt-Nd1-DdCBE injected follicles	60	33 (55.0% per follicles)	20 (33.3% per follicles; 60.6% per COCs)	18 (30.0% per follicles; 90% per MII oocytes)	14 (23.3% per follicles; 77.8% per fertilized oocytes)	6 (10.0% per follicles; 42.9% per 2-cell embryos)

COC, cumulus-oocyte complex; DdCBE, DddA-derived cytosine base editors; MII, metaphase II stage.

MATERIALS AND METHODS

Plasmids generation and the RVD repeats assembly

TALE-based DdCBEs vectors were synthesized in Sangon Biotech, which is composed of mitochondrial localization sequence, N-terminal, C-terminal, one kind of four split DddA halves, and uracil glycosylase inhibitor (UGI)-coding sequences, and four vectors were designed for each site according to the two different split DddA halves (G1333-N, G1333-C, G1397-N, and G1397-C) and different orientations. The detailed amino acid information of each DdCBE element is presented in Table S2. The detailed TALEN binding sequence of mt-Nd1 and mt-Nd5 are shown in Table S3.

Cell culture, transfection, and DdCBEs pairs optimization

Neuro-2A cells were ordered from the Chinese Academy of Sciences and cultured with MEM medium (Life Technologies) supplement with 10% fetal bovine serum (Gibco), 1% sodium pyruvate (Gibco), 1% nonessential amino acids, and 1% penicillin/streptomycin solution (Life Technologies) under 5% CO_2 at 37°C. A 3-μg mixture of DdCBEs was transfected to Neuro-2A cells using Lipofectamine 3000 (Life Technologies) according to the manufacturer's manual. G418 (750 μg/mL) was added 1 day posttransfection for 4 days. Six days posttransfection, cells were collected and DNA was extracted using DNaesy Blood & Tissue Kit (Qiagen) followed by Sanger sequencing or next-generation target sequencing to select the best pair for subsequent *in vitro* transcription (IVT).

In vitro transcription transcription

DddA fused mito-TALEN plasmids containing T7 promoter were linearized with NotI (NEB) endonuclease, followed by purification with 1.2% electrophoresis gel. Then, the purified product was used as the template for IVT using mMESSAGE T7 ULTRA kit (Life Technologies) according to the manufacturer's manual. Both halves of TALEN mRNA were purified using a MEGAclear kit (Life Technologies) and eluted in RNase-free water for germ cell microinjection.

Animals

All of the mice used in this study were ordered from Beijing Vital River Laboratory Animal Technology and maintained at 23°C under a 12-h:12-h light-dark schedule. C57/B6J mice were used for zygote retrieval and ICR or B6D2F1 mice were used for follicle culture *in vitro*. All of the experimental procedures were performed in accordance with the Institutional Animal Care or Research Ethics Committee from Shanghai Jiao Tong University School of Medicine.

Zygote collection

For pronuclear embryos collection, 6-week-old female mice (C57/B6) were superovulated by intraperitoneal injection of 10 IU of pregnant mare's gonadotrophin (Ningbo Hormone Products) and 10 IU human chorionic gonadotropin (hCG) (Ningbo Hormone Products) at a 48-h interval. Then, female mice were crossed with males. Fertilized embryos with two pronuclei were collected from the oviducts of mice with vaginal plug 20 h post-hCG administration in M2 media. Cumulus mass was removed in 70 μg/mL bovine testicular hyaluronidase for microinjection. After 1 h of recovery, mixed forward and reverse TALENs-based DdCBE with a final concentration of 150 ng/μL was injected into the cytoplasm of the pronuclear embryos, followed by culturing in potassium-supplemented simplex optimised medium at 37°C under 5% CO_2 in air under mineral oil.

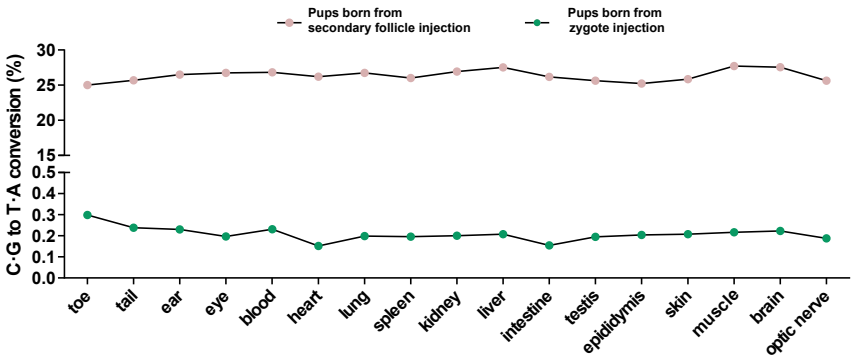

Figure 5. MtDNA heteroplasmy of tissues derived from founder mice produced by zygote or follicle mtDNA base editing strategy

Heteroplasmy levels of mtDNA in different tissues of male founders born from zygote injection (N = 5) and secondary follicle injection (N = 1).

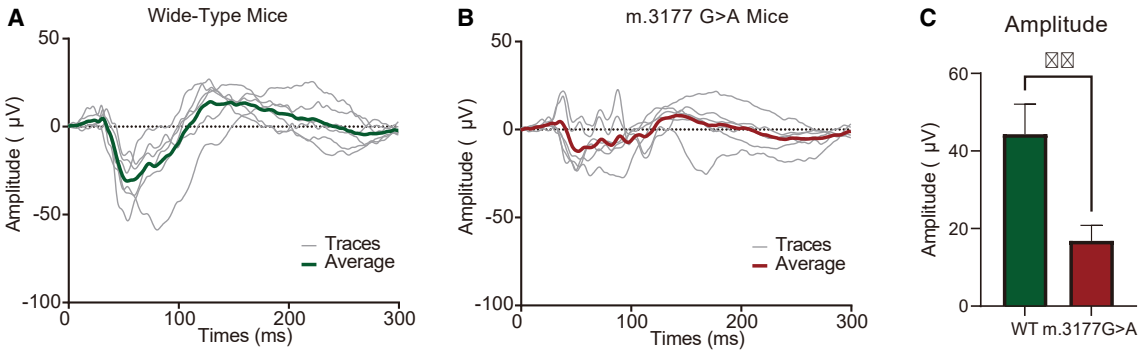

Figure 6. Evaluation of visual evoked potential results of WT and m.3177 G>A mice

(A and B) The evaluation of visual evoked potential waveforms of WT (A) and m.3177 G>A mice (B). Each group contained 3 mice. (C) Comparison of amplitude of WT and m.3177 G>A mice. Significance was calculated with unpaired 2-tailed Student's t test (**p < 0.01). The error bars represent the standard error of the mean.

Follicle culture *in vitro*

A detailed method for follicle culture *in vitro* has been described previously.[20] In brief, secondary follicles with a diameter between 105 and 125 μm were collected from 12-to 14-day-old ICR or B6D2F1 female mice using L-15 media (Gibco) supplemented with 2% polyvinylpyrrolidone (PVP, Sigma) and 10% fetal bovine serum (Gibco). Notably, PVP's molecular weight of 360,000 is crucial for optimal follicle growth.[20] Isolated follicles with intact shape and high density of granulosa cells were selected for further microinjection and *in vitro* culture. A short time (∼5 min) of collagenase treatment was performed to weaken the follicle to allow the microinjection. After 1 h of recovery, follicles were microinjected with a mixture of left and right halves of DdCBE mRNA with a final concentration of 150 ng/μL. After microinjection, another 20–25 min of collagenase treatment was performed to totally remove the follicle wall for better growth *in vitro*.[20] Follicles were cultured in α-MEM supplemented with 5% fetal bovine serum, 1% GlutaMax (Gibco), 2% PVP, 0.1% penicillin/streptomycin (Gibco), 150 μM 2-*O*-α-D-glucopyranosyl-L-ascorbic acid (AA2G, Tokyo Chemical Industry) and 100 mU/mL follicle-stimulating hormone (FSH, Gonal-F). The culture incubator was set at 37°C, 100% humidity, and 5% CO_2 in air, and approximately half of the media was refreshed every other day. After ∼11 days of culture, COCs were harvested for final maturation, with α-MEM supplemented with 5% fetal bovine serum, 1% GlutaMax, 0.1% penicillin/streptomycin, 150 μM AA2G, 100 mU/mL FSH, 1,200 mU/mL recombinant hCG (VIDREL) and 10 ng/mL epidermal growth factor (Sigma). The oocytes were kept in an *in vitro* maturation medium for 17 h before *in vitro* fertilization. Expanded COCs were fertilized in human tubal fluid (Merck) medium with epididymal sperm from 8-week-old B6D2F1 males. Zygotes with two pronuclei 6 h postsperm addition were considered to be normal fertilization. For embryo transfer, two-cell stage embryos derived from normal two pronuclei zygotes were transferred into the oviducts of pseudopregnant females at 0.5 days post coitum (dpc).

DNA extraction

Genomic DNA was extracted and the efficiency of mtDNA mutation was tested 3–4 days postinjection either using Sanger sequencing, target deep sequencing, or the digital PCR quantification for extremely rare mutations. For single-germ cell genome DNA extraction, follicles were digested with 0.5% trypsin (Gibco), 0.1% collagenase type I (Worthington), 0.1% DNase I (Sigma), and 1 mM EDTA (Solarbio) in an incubator at 37°C for 10 min, and then, granulosa cells were removed mechanically to isolate single oocytes. Oocytes or embryos were collected individually and rinsed three times in 0.4% BSA solution, and then put separately into 5μL QuickExtract DNA Extraction Solution for digestion following the manufacturer's instructions. For cells and tissues, total genome DNA was extracted using a DNaesy Blood & Tissue Kit (Qiagen) according to the manufacturer's instructions.

Digital PCR

Primers and probes were ordered from IDT, and detailed information is presented in Table S4. Briefly, a 5-μL single-cell sample was added with 10 μL DNase-free double-distilled H_2O and 2-μL mixture was used as a template for PCR amplification. Reaction droplets were prepared from a total 20-μL PCR mix by QX200TM droplet digital PCR instrument's droplet generator and amplified on the Bio-Rad T100 PCR instrument (95°C, 10 min; 94°C, 30 s; 60°C, 1 min, 40 cycles; 98°C, 10 min). After PCR amplification, the fluorescence signal of FAM (WT copies) and HEX (mutant copies) in each droplet was read by the QX200 Droplet Reader and analyzed by QuantaSoft. To validate the sensitivity and accuracy of digital PCR, edited and untreated zygotes were tested and compared. The results indicated that digital PCR is sensitive enough to capture the rare mutant mtDNA within the zygotes (Figure S6A), When we compared the results of the same sample sequenced by digital PCR and next-generation sequencing (NGS), respectively, we found that the data show no difference between these two groups, which means that data from the digital PCR and the NGS were equivalent (Figure S6B).

Next generation sequencing

A total of 100 ng genome DNA extracted from cells or tissues or all lysates for single cells were used for first-round PCR using Phanta Flash DNA Polymerase (Vazyme) to amplify target sequences with

primers containing barcodes and Illumina adapters. A 1-μL product was used for second-round PCR using index primers (Vazyme). After second-round PCR, samples with different barcodes and indexes were mixed, purified by gel extraction using the QIAquick Gel Extraction Kit (Qiagen), and quantified using the Qubit ssDNA HS Assay Kit (Thermo Fisher Scientific).

Sequencing was performed on the Illumina NovaSeq 6000 platform. Primers for targeted sequencing are listed in Table S4. Quality control was performed for the sequencing data by fastp (version 0.23.2) using default parameters. Then, sequencing reads were demultiplexed using fastq-multx (version 1.4.1) with the barcoded PCR primers. Next, the editing frequencies of the on-target sites were calculated by output file from batch analysis with CRISPResso2 (version 2.0.32), and statistics were generated using in-house scripts with R (version 4.2.1).

Whole-mtDNA sequencing

The whole mtDNA was amplified as two overlapping 8-kb fragments by long-range PCR, and the sequence information of the primers is shown in Table S4. The PCR products were purified by QIAquick Gel Extraction Kit (Qiagen) and used as input for constructing libraries using TruePrep DNA Library Prep Kit V2 for Illumina (Vazyme). The libraries were purified using DNA clean beads and quantified using the Qubit ssDNA HS Assay Kit (Thermo Fisher Scientific) before performing the deep sequencing.

To analyze NGS data from whole mitochondrial genome sequencing, we first mapped the qualified reads to the human mitochondrial reference genome (hg19) by BWA (version 0.7.12) with mem –M, and then generated BAM files with SAMtools (version 1.9). Positions with conversion rates $\geq$0.1% were identified among all of the cytosines and guanines in the mitochondrial genome using the REDItool-Denovo.py script from REDItools (version 1.2.1).

Off-target analysis

Mitochondrial genome-wide off-target analysis was performed using the method described previously.[11] Sites with C·G to T·A frequencies >1% in untreated samples were excluded. For off-target analysis of each sample, sites with a mutant rate of <1% were excluded due to the sensitivity of NGS. For average off-target analysis, the average C·G to T·A conversion was calculated for each sample by using the total number of T and A reads in all nontarget C·G base pairs to divide by the total number of reads that covered all nontarget C·G base pair.

Visual evoked potential (VEP)

Following 8 h of dark adaptation timed to specific test periods, mice were anesthetized and their pupils dilated. Full-field stimulators have been used to illuminate the entire visual field of the mice to ensure that the stimulating light adequately activates the visual system. Each eye received 60 flashes of 1 cd s/m^2 white light at 1 Hz. Data analysis focused on the N1 (most prominent negative peak) amplitudes. Throughout the procedure, dark adaptation, body temperature, and corneal moisture were meticulously maintained, and electrode impedances stayed within designated ranges.

Statistical analysis

In this study, we assessed the normality of the data using the Shapiro-Wilk test. For independent samples, if the data satisfied the assumptions of normality, we conducted an unpaired Student's t test to analyze the differences between groups. However, if the data did not meet the assumptions of normality or equal variances, we used the Mann-Whitney *U* test. For paired samples, when comparing digital PCR and NGS, we used a paired Student's t test to examine the differences.

DATA AND CODE AVAILABILITY

The datasets used in the present study are available and will be deposited into the public database if necessary.

SUPPLEMENTAL INFORMATION

Supplemental information can be found online at https://doi.org/10.1016/j.omtn.2024.102170.

ACKNOWLEDGMENTS

We thank Prof. Xingxu Huang from Shanghai Tech University, and Prof. Yunbo Qiao from Shanghai Institute of Precision Medicine for their critical reading of our manuscript, and we also thank Prof. Aaron. J. Hsueh from Stanford University for his assistance in excellent language editing. This work was supported by the Science and Technology Commission of Shanghai Municipality (21JC1403900).

AUTHOR CONTRIBUTIONS

L.S. and Y.K. conceived the idea and designed the project. H.W., J.Q., X.J., and S.Z. generated the constructs and selected the optimal DddAtox pairs. Q.X., H.L., and W.Y. set up the follicle culture system. H.W. and J.L. performed the microinjections. Q.X. isolated the single oocytes or embryos and extracted the genomic DNA. Q.X. performed the digital PCR test and constructed the library for NGS. H.W. performed the Illumina sequence data analysis. C.X. performed the VEP experiments. L.S. wrote the manuscript, with input from all of the authors. L.S., Q.L., and Y.K. supervised the project.

DECLARATION OF INTERESTS

The authors declare no competing interests.

REFERENCES

1. Newmeyer, D.D., and Ferguson-Miller, S. (2003). Mitochondria: releasing power for life and unleashing the machineries of death. Cell *112*, 481–490.
2. Starkov, A.A. (2008). The role of mitochondria in reactive oxygen species metabolism and signaling. Ann. N. Y. Acad. Sci. *1147*, 37–52.
3. Silva-Pinheiro, P., and Minczuk, M. (2022). The potential of mitochondrial genome engineering. Nat. Rev. Genet. *23*, 199–214.
4. Lightowlers, R.N., Taylor, R.W., and Turnbull, D.M. (2015). Mutations causing mitochondrial disease: What is new and what challenges remain? Science *349*, 1494–1499.
5. Sharma, P., and Sampath, H. (2019). Mitochondrial DNA Integrity: Role in Health and Disease. Cells *8*, 100.

6. Yang, H., Wang, H., and Jaenisch, R. (2014). Generating genetically modified mice using CRISPR/Cas-mediated genome engineering. Nat. Protoc. *9*, 1956–1968.

7. Chernega, T., Choi, J., Salmena, L., and Andreazza, A.C. (2022). Mitochondrion-targeted RNA therapies as a potential treatment strategy for mitochondrial diseases. Mol. Ther. Nucleic Acids *30*, 359–377.

8. Komor, A.C., Kim, Y.B., Packer, M.S., Zuris, J.A., and Liu, D.R. (2016). Programmable editing of a target base in genomic DNA without double-stranded DNA cleavage. Nature *533*, 420–424.

9. Gaudelli, N.M., Komor, A.C., Rees, H.A., Packer, M.S., Badran, A.H., Bryson, D.I., and Liu, D.R. (2017). Programmable base editing of A·T to G·C in genomic DNA without DNA cleavage. Nature *551*, 464–471.

10. Gammage, P.A., Moraes, C.T., and Minczuk, M. (2018). Mitochondrial Genome Engineering: The Revolution May Not Be CRISPR-Ized. Trends Genet. *34*, 101–110.

11. Mok, B.Y., de Moraes, M.H., Zeng, J., Bosch, D.E., Kotrys, A.V., Raguram, A., Hsu, F., Radey, M.C., Peterson, S.B., Mootha, V.K., et al. (2020). A bacterial cytidine deaminase toxin enables CRISPR-free mitochondrial base editing. Nature *583*, 631–637.

12. Cho, S.I., Lee, S., Mok, Y.G., Lim, K., Lee, J., Lee, J.M., Chung, E., and Kim, J.S. (2022). Targeted A-to-G base editing in human mitochondrial DNA with programmable deaminases. Cell *185*, 1764–1776.e12.

13. Guo, J., Zhang, X., Chen, X., Sun, H., Dai, Y., Wang, J., Qian, X., Tan, L., Lou, X., and Shen, B. (2021). Precision modeling of mitochondrial diseases in zebrafish via DdCBE-mediated mtDNA base editing. Cell Discov. *7*, 78.

14. Qi, X., Chen, X., Guo, J., Zhang, X., Sun, H., Wang, J., Qian, X., Li, B., Tan, L., Yu, L., et al. (2021). Precision modeling of mitochondrial disease in rats via DdCBE-mediated mtDNA editing. Cell Discov. *7*, 95.

15. Qi, X., Tan, L., Zhang, X., Jin, J., Kong, W., Chen, W., Wang, J., Dong, W., Gao, L., Luo, L., et al. (2023). Expanding DdCBE-mediated targeting scope to aC motif preference in rat. Mol. Ther. Nucleic Acids *32*, 1–12.

16. Lee, H., Lee, S., Baek, G., Kim, A., Kang, B.-C., Seo, H., and Kim, J.S. (2021). Mitochondrial DNA editing in mice with DddA-TALE fusion deaminases. Nat. Commun. *12*, 1190.

17. Guo, J., Chen, X., Liu, Z., Sun, H., Zhou, Y., Dai, Y., Ma, Y., He, L., Qian, X., Wang, J., et al. (2022). DdCBE mediates efficient and inheritable modifications in mouse mitochondrial genome. Mol. Ther. Nucleic Acids *27*, 73–80.

18. Chen, X., Liang, D., Guo, J., Zhang, J., Sun, H., Zhang, X., Jin, J., Dai, Y., Bao, Q., Qian, X., et al. (2022). DdCBE-mediated mitochondrial base editing in human 3PN embryos. Cell Discov. *8*, 8.

19. Wei, Y., Xu, C., Feng, H., Xu, K., Li, Z., Hu, J., Zhou, L., Wei, Y., Zuo, Z., Zuo, E., et al. (2022). Human cleaving embryos enable efficient mitochondrial base-editing with DdCBE. Cell Discov. *8*, 7.

20. Ota, S., Ikeda, S., Takashima, T., and Obata, Y. (2021). Optimal conditions for mouse follicle culture. J. Reprod. Dev. *67*, 327–331.

21. Wei, Y., Li, Z., Xu, K., Feng, H., Xie, L., Li, D., Zuo, Z., Zhang, M., Xu, C., Yang, H., and Zuo, E. (2022). Mitochondrial base editor DdCBE causes substantial DNA off-target editing in nuclear genome of embryos. Cell Discov. *8*, 27.

22. St John, J.C., Facucho-Oliveira, J., Jiang, Y., Kelly, R., and Salah, R. (2010). Mitochondrial DNA transmission, replication and inheritance: a journey from the gamete through the embryo and into offspring and embryonic stem cells. Hum. Reprod. Update *16*, 488–509.

23. Thundathil, J., Filion, F., and Smith, L.C. (2005). Molecular control of mitochondrial function in preimplantation mouse embryos. Mol. Reprod. Dev. *71*, 405–413.

24. Shoubridge, E.A., and Wai, T. (2007). Mitochondrial DNA and the mammalian oocyte. Curr. Top. Dev. Biol. *77*, 87–111.

25. Telfer, E.E., and Andersen, C.Y. (2021). In vitro growth and maturation of primordial follicles and immature oocytes. Fertil. Steril. *115*, 1116–1125.

26. Morohaku, K., Tanimoto, R., Sasaki, K., Kawahara-Miki, R., Kono, T., Hayashi, K., Hirao, Y., and Obata, Y. (2016). Complete *in vitro* generation of fertile oocytes from mouse primordial germ cells. Proc. Natl. Acad. Sci. USA *113*, 9021–9026.

27. Zhen, X., Wu, B., Wang, J., Lu, C., Gao, H., and Qiao, J. (2015). Increased Incidence of Mitochondrial Cytochrome C Oxidase 1 Gene Mutations in Patients with Primary Ovarian Insufficiency. PLoS One *10*, e0132610.

28. Kirillova, A., Smitz, J.E.J., Sukhikh, G.T., and Mazunin, I. (2021). The Role of Mitochondria in Oocyte Maturation. Cells *10*, 2484.